Journal of the Korean Physical Society, Vol. 24, No. 6, December 1991, pp. 460~466

Analysis of Stimulated Cyclotron Resonance Scattering of a Circularly Polarized Pump by a Relativistic Electron Beam

Tae Hun CHUNG

Department of Physics, Dong-A University, Pusan 604-714

(Received 13 June 1991, in final form 10 October 1991)

The scattering of a right-handed circularly polarized pump wave by a relativistic electron beam with a finite temperature is described in terms of the coupled Maxwell and linear fluid equations. The gain calculations are performed by the use of the Madey theorem and compared with other results. The effects of the electron beam energy and the strength of the axial guide field on the major characteristics of the system are investigated for the amplifier configuration.

I. INTRODUCTION

In this study, the interaction of a high frequency right-handed circularly polarized (RHCP) pump wave with a magnetized electron beam is analyzed. It has been known that the stimulated Raman growth rate is enhanced when the plasma is magnetized, and the frequency of the pump wave is tuned near the electron cyclotron frequency.[1,2] This phenomenon has some implications to the study of an electromagnetically pumped free-electron laser (FEL) with an axial guide magnetic field[3,4] since the equivalence of the FEL and stimulated scattering mechanisms has been shown.[5]

The latest proposal to shorten the FEL wavelength suggests an optical wiggler.[6] The use of a short wavelength electromagnetic wave as the wiggler field would allow a substantial reduction of the beam energy necessary for obtaining any given laser frequency. FEL operation at lower beam energy has many major technological implications, including the availability of alternate accelerator technologies, a reduced activation and radiation hazard, a reduced system size, and a reduced shielding requirement.[6] This optical wiggler (sometimes called an electromagnetic wiggler) may be produced either by a first-stage FEL working at low energy or by an external powerful pulsed laser. The former technique is called two-stage FEL and has been already explored at Santa Barbara where a 700 μm optical wiggler generated by a 6 MeV electron beam should generate a second-stage FEL at 1 μm.[7,8] The latter technique has been studied theoretically[9] and still has to be proven to be achievable and useful. The pump wave considered in this study corresponds to the light either from a first-stage FEL or from a powerful pulsed laser with a high degree of frequency stability.

A two-stage optically pumped FEL has a low growth rate. The intrinsic efficiency is also typically small, but efficiency enhancement is possible if the first- and second-stage radiation fields are strong enough to produce electron trapping in the ponderomotive wave. The electron beam quality must be very high for sucessful operation of an efficient two-stage FEL at short wavelength.[10]

The photon scattering by electrons gyrating in the magnetic field when the pump is tuned at the cyclotron frequency of the electron is called cyclotron resonance scattering. In a fusion plasma, this mechansim may prevent the efficient heating of the plasma by RF sources.[11]

In this study, a three-wave parametric process in which a scattered electromagnetic wave grows as a result of the interaction between a pump wave and a beam cyclotron mode is analyzed via the Maxwell fluid equations. The growth rate of the instability is calculated, and the gain coefficient is formulated according to the Madey theorem[12] and reformulated into a more useful form for a comparison. Finally, the intrinsic efficiency of energy extraction is estimated for the amplifier configuration.

This analysis is performed in the relativistic region and includes the effect of the electron beam temperature (axial energy spread). The concept of fluid pressure is used to treat the effect of beam thermal spread. Analyses dealing with the phenomena considered in this study can be found elsewhere,[1-4] but the merits of our approach may be its simpler physical picture and the straightforward calculation.

Usually, the electron beam propagating in a uniform axial guide field is assumed to be a solid beam or annular beam.[13] In the present analysis, a solid electron beam is considered as in Fig. 1.

The magnitude of the self field in the z-direction for a uniform density and a rigid rotor configuration is written as[14]

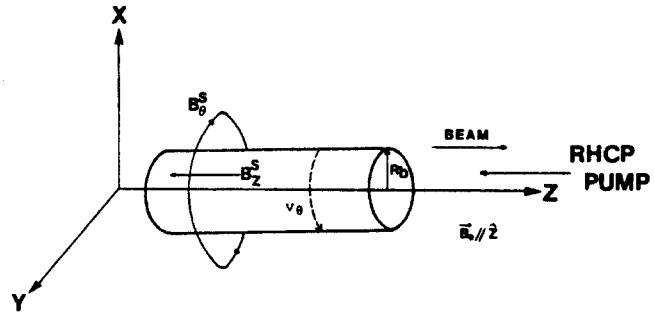

Fig. 1. Model Configuration. B_θ^s and B_z^s represent the self field in the θ and z directions, respectively.

$$\frac{B_z^s(r=0)}{B_0} = \frac{\omega_e^2 R_b^2}{c^2} \frac{\omega_p^2/2\Omega_e}{\omega_e} \tag{1}$$

where $\omega_e^{\pm} = \frac{\Omega_e}{2\gamma}[1\pm(1-\frac{2\omega_p^2}{\gamma\Omega_e^2})^{1/2}]$

is the rotation frequency. Note that Eq. (1) is valid only for a uniform density and a rigid rotor configuration.

When $\frac{v_\theta(R_b)}{c} \ll 1$ and $|\frac{\omega_p^2}{2\Omega_e}| \leq |\omega_e|$, we have

$$B_0 \gg B_z^s \ (r=0). \tag{2}$$

Thus, we can neglect the axial diamagnetic effect. Practically, the cross-sectional dimension of the electron beam is much less than that of the laser beam. It is also much less than the distance characterizing the transverse variation in the cirularly polarized pump wave. If we denote the filling factor F as

$$F = \frac{A_b}{A_\omega} = \frac{\pi R_b^2}{\pi R_r^2} \tag{3}$$

where R_r is the radius of the scattered radiation, then generally $F \ll 1$. Thus, the system can be assumed to be uniform in the transverse direction, and we can carry out the calculations for uniform density beams with infinite transverse dimension. Therefore the influence of finite radial geometry on the growth rate of the parametric instability cannot be examined in this analysis.

The spatial growth rate, gain, and efficiency depend on the energy of the relativistic electron beam and on the axial guide field. We will show quantitatively how these parameters affect the major characteristics of the system (growth rate, gain, and efficiency).

II. ANALYSIS

The pump field within the plasma is taken to have the form

$$E_0(t) = E_0 \cos \omega_0 t \ \hat{e}_x - E_0 \sin \omega_0 t \ \hat{e}_y. \tag{4}$$

The electron orbits in the presence of B_o and E_o (t) are given by[1]

$$v_0 = v_0 \hat{e}_z + V_0 \ (\hat{e}_x \sin \omega_0 t + \hat{e}_y \cos \omega_0 t) \tag{5}$$

where

$$V_0 = \frac{q}{m\gamma_0} \frac{E_0}{\omega_0 - \frac{\Omega_e}{\gamma_0}},$$

$$\omega_0 = \frac{1}{\gamma_0}[\frac{\Omega_e}{\gamma_0} + \sqrt{(\frac{\Omega_e}{\gamma_0})^2 + \frac{4\omega_p^2}{\gamma_0^2}}].$$

We choose to perform the analysis in a reference frame in which the pump's wavenumber along the z-axis vanishes (for supraluminous waves, such a transformation is always possible). However, in a conventional laboratory frame, the velocity components of the electron trajectories are

$$v_0^2 + V_0^2 = c^2(1-\gamma_0^{-2}),$$

$$V_0 = \frac{q}{m\gamma_0} \frac{E_o \ (1+k_0 v_0/w_0)}{w_0 + k_0 v_0 - \Omega_e/\gamma_0} \tag{6}$$

where k_0 is the wavenumber of the incoming RHCP wave in laboratory frame such as $E_0 = E_0[-\hat{e}_x \sin(k_0 z + w_0 t) + \hat{e}_y \cos(k_0 z + w_0 t)]$. The solutions of Eq. (6) fall into two categories: the so-called group-I orbits apply when $\Omega e < \gamma_0(w_0 + k_0 v_0)$ (below resonance), and group-II orbits result when $\Omega_e > \gamma_0 \ (w_0 + k_0 v_0)$ (above resonance). It should be noted that the parameter region considered for the numcrical illustration (Section IV) is restricted to group I.

Using the Coulomb gauge, the transverse component of the Maxwell wave equation is

$$(\frac{\partial^2}{\partial z^2} - \frac{1}{c^2}\frac{\partial^2}{\partial t^2}) A_\perp = -\frac{4\pi}{c} FJ. \tag{7}$$

With the linearization of the perturbed (primed) quantities, Eq. (7) can be written as

$$(\frac{\partial^2}{\partial z^2} - \frac{1}{c^2}\frac{\partial^2}{\partial t^2}) A'_\perp = -F\frac{4\pi q}{c}(n_0 v'_\perp + n' v_{\perp 0}). \tag{8}$$

The perturbed perpendicular velocity is written as[5]

$$v'_\perp = \frac{qi}{m\gamma_0} \frac{1}{\omega - kv_0 \mp \frac{\Omega_e}{\gamma_0}} E'_\perp, \tag{9}$$

and we note that

$$E'_\perp = -\frac{1}{c}\frac{\partial A'}{\partial t} = \frac{i\bar{\omega}}{c} A'_\perp \tag{10}$$

Thus,

$$F\frac{4\pi q n_0}{c} v'_\perp = -F\frac{w_p^2}{\gamma_0 c^2} \frac{\bar{\omega}}{\bar{\omega} \mp \frac{\Omega_e}{\gamma_0}} A'_\perp \tag{11}$$

where

$\bar{\omega}=\omega-kv_0$.

Thus, we can write Eq. (8) as

$$\frac{\partial^2}{\partial z^2}-\frac{1}{c^2}\frac{\partial^2}{\partial t^2}-\frac{F\omega_p^2}{\gamma_0 c^2}\frac{\bar{\omega}}{\bar{\omega}\mp\frac{\Omega_e}{\gamma_0}}\Big) A_\perp'$$

$$=-\frac{4\pi qE}{c}n'v_{\perp 0} \tag{12}$$

where $v_{\perp 0}=V_0\ (\hat{e}_x \sin w_0t+\hat{e}_y \cos w_0t)$.

The scattered fields are taken to be perturbed quantities having the general form

$$G'(z,t)=\sum_{n=-\infty}^{\infty} G_n'(k)e^{ikz-iw_nt} \tag{13}$$

where $G_n'(k)$ is the Fourier coefficient, $w_n=\omega+n\omega_0$, and k is the wave number of the n-th mode.

Equation (12) with the linearized continuity equation and Poisson's equation yields

$$A_{xn}'=\frac{F2\pi qV_0}{c}(n_{n+1}'-n_{n-1}')[-k^2+$$

$$\frac{\omega_n^2}{c^2}-\frac{F\omega_p^2}{\gamma_0 c^2}\frac{\bar{\omega}}{\bar{\omega}\mp\frac{\Omega_e}{\gamma_0}}]^{-1}, \tag{14a}$$

$$A_{yn}'=-\frac{F2\pi qV_0}{c}(n_{n+1}'n_{n-1}')[-k^2+$$

$$\frac{\omega_n^2}{c^2}-\frac{F\omega_p^2}{\gamma_0 c^2}\frac{\bar{\omega}}{\bar{\omega}\mp\frac{\Omega_e}{\gamma_0}}]^{-1}, \tag{14b}$$

$$E_{zn-1}'=-\frac{i4\pi q}{k}n_{n-1}'. \tag{14c}$$

Then, the amplitude of the electrostatic wave can be written in terms of the amplitude of the electromagnetic wave,

$$E_{zn-1}'=\frac{iR_n^+}{FkV_0\omega_n}E_n'^+ \tag{15}$$

where

$$R_n^\pm=\omega_n^2-k^2c^2-\frac{F\omega_p^2}{\gamma_0}\frac{\bar{\omega}_n}{\bar{\omega}_n\mp\frac{\Omega_e}{\gamma_0}}$$

$$E_n'^\pm=E_{xn}'\pm iE_{yn}',$$

and $\pm$ denotes RHCP and LHCP, respectively.

The perturbed longitudinal component of the momentum transfer equation, including the temperature effect, is written as

$$\gamma_0^3\Big(\frac{\partial}{\partial t}+v_0\frac{\partial}{\partial z}\Big)v_z'=\frac{q}{m}[E_z'+\frac{1}{c}(v\times B)_z']-\frac{3k_BT}{n_0m}\frac{\partial n'}{\partial z}. \tag{16}$$

Performing a Fourier analysis, Eq. (16) is expressed as

$$-i\gamma_0^3(\omega_n-kv_0)v_{zn}'=\frac{q}{m}[E_{Zn}'+(\frac{-iV_0k}{2})(\frac{E_{xn+1}'}{\omega_{n+1}}-\frac{E_{xn-1}'}{\omega_{n-1}})$$

$$+\frac{V_0k}{2}(\frac{E_{yn+1}'}{\omega_{n+1}}+\frac{E_{yn-1}'}{\omega_{n-1}})]-\frac{3k_BT}{n_0m}ikn_n'. \tag{17}$$

From the linearized continuity equation, we have

$$v_{zn}'=\frac{\omega_n-kv_0}{n_0k}n_n'. \tag{18}$$

Equations (14c), (15), (17), and (18) yield

$$E_{zn}'=\tilde{A}_nE_{n+1}^+ \tag{19}$$

where

$$\tilde{A}_n=\frac{-i[\bar{\omega}_n^2+(3/\gamma_0^3)(k\lambda_D)^2\omega_p^2]\gamma_0^3}{F\omega_p^2kV_0\omega_{n+1}}R_{n+1}^++\frac{iV_0k}{2\omega_{n+1}}$$

and

$\bar{\omega}_n=\omega_n-kv_0$.

From Eqs. (15) and (19),

$$R_n^+=ikV_0\omega_nF\tilde{A}_{n-1}. \tag{20}$$

Thus, the dispersion relation for the RHCP wave is obtained as

$$w_n^2-k^2c^2-\frac{F\omega_p^2\bar{\omega}_n}{\gamma_0(\bar{\omega}_n-\frac{\Omega_e}{\gamma_0})}-\frac{1}{2}\frac{F\omega_p^2V_0^2k^2}{\gamma_0^3(\bar{\omega}_{n-1}^2+\frac{3k^2\lambda_D^2\omega_p^2}{\gamma_0^3})-\omega_p^2}=0 \tag{21}$$

Solving Eq. (21) gives

$$Im(\omega_n)\simeq\frac{1}{2}\mid\frac{V_0}{c}\mid F\tfrac{1}{2}ck[\frac{\sqrt{1-3(k\lambda_D)^2}}{\gamma_0}\frac{\omega_p}{2\omega_n+\frac{\Omega_e}{\gamma_0}}]^{1/2} \tag{22a}$$

$$Re(\omega_n)\simeq\frac{\Omega_e}{(1-\frac{V_0}{c})\gamma_0}, \tag{22b}$$

$$K\simeq\frac{\Omega_e}{(1-\frac{V_0}{c})\gamma_0c}, \tag{22c}$$

where we have assumed that

$Re(\omega_n)\gg Im(\omega_n)$.

We note that Eq. (22b) is approximated as

$$Re(\omega_n)\simeq 2\Omega_e\gamma_0, \tag{23}$$

and $Re(\omega_n)$ is the frequency for the scattered *em* radiation (i.e., $\omega_s=Re(\omega_n)=2\pi c/\lambda_s$).

III. GAIN CALCULATION

The Lorentz equation is written as

$$mc^2 \frac{d\gamma}{dt} = -eE_l \cdot v \tag{24}$$

where E_l is the electric field of the electromagnetic wave and can be written as

$$E_l = E_l[\hat{e}_x \cos(kz - \omega_n t + \phi) + \hat{e}_y \sin(kz - \omega_n t + \phi)] \tag{25}$$

where ϕ is the phase angle between the electron and the electromagnetic wave. The first-order perturbation equation of γ caused by the electromagnetic wave is

$$mc^2 \frac{d\gamma_1}{dt} = -eE_l \cdot v_0$$
$$= -eV_0 E_l \sin[kz - (\omega_n - \omega_0)t + \phi]. \tag{26}$$

Integrating Eq. (26) in the interaction region [0, L], we have

$$\gamma_1 = \frac{eV_0 E_l}{mc^2 V_0} \frac{\cos(\Delta kL + \phi) - \cos\phi}{\Delta k} \tag{27}$$

where $\Delta k = k - \frac{\omega_n - \omega_0}{v_0}$

Squaring γ_1 and averaging over ϕ gives

$$<\gamma_1^2> = \frac{L^2}{2} \left(\frac{eV_0 E_l}{mc^2 V_0}\right)^2 \frac{\sin^2 U}{U^2}$$

where $U = \frac{L}{2}\Delta k$. (28)

According to the Madey theorem,[12] we obtain a second-order perturbation of γ,

$$<\gamma_2> = \frac{1}{2} \frac{d}{dr} <\gamma_1^2>. \tag{29}$$

The gain is formulated as[16]

$$G = - \frac{<\gamma_2> mc^2 I/e}{\frac{1}{8\pi} E_l^2 c A_\omega} \tag{30}$$

where A_ω is the area of the optical wave and I is the electron beam current ($I = ne\, v_0\, A_b$).
The final formula for gain is

$$G = \frac{F}{4} \frac{\omega_p^2 L^3 C(\omega_n - \omega_0)}{v_0^4 \gamma_0^3} \left(\frac{V_0}{c}\right)^2 \frac{d}{dU} \left(\frac{\sin^2 U}{U^2}\right)$$
$$= \frac{4}{\pi^3} \frac{\omega_p^2 L^3 Fk}{\beta_z^3 c^2 \gamma_0^3} \left(\frac{V_0}{c}\right)^2 \tag{31}$$

where we have used the maximum value of

$$\frac{d}{dU} \frac{\sin^2 U}{U^2} \text{ as } \frac{16}{\pi^3} \text{ at } U^2 = 1.303.$$

It should be noted that this formula is only valid for the small signal region.

The undulator parameter K for the electromagnetic wiggler which specifies the resonance condition can be written as

$$K = \frac{e\lambda_p E_0}{2\pi mc^2} \tag{32}$$

where $\lambda_p = \frac{2\pi c}{w_0}$

We can write this parameter in terms of the pump intensity S ($= c\varepsilon_0 E_0^2$);

$$K^2 = \frac{e\lambda_p^2 S}{\pi mc^2 I_A} \tag{33}$$

where I_A is the Alfven current, $I_A = 4\pi\varepsilon_0 \frac{mc^3}{e} = 17000$ Amp.

We note that

$$\frac{V_0}{c} = \frac{K}{\gamma} \tag{34}$$

and the interaction length L is half the pulse length of the undulator laser L_p. The pulse length L_p ($= N\lambda_p$; N is the number of undulator periods) has been chosen to take the value $L_p = 4\, Z_p$ (where Z_p is the Rayleigh range).[9]

Using the resonance condition

$$\lambda_s = \frac{\lambda_p}{4\gamma^2}(1 + K^2), \tag{35}$$

the gain formula can be rearranged as

$$G = \frac{e^2}{\varepsilon_0 m^2 c^5} \frac{\lambda_s^{3/2}}{\lambda_p 1/2} \frac{L_p^3}{\sigma_e} S \frac{I}{I_A} \frac{d}{dU} \frac{\sin^2 U}{U^2} \tag{36}$$

where I is the total current and σ_e is the electron beam area. The gain formula of Eq. (36) is more adequate for estimating gain in terms of experimental parameters and is well in accord with previous results.[9,17]

This analysis has been restricted to group I orbits far from the magnetoresonance.

IV. NUMERICAL ILLUSTRATION

In this section, obtained equations are numerically evaluated. In the first place, we investigate the effect of the electron beam temperature on the spatial growth rate of the scattered RHCP electromagnetic wave. It has been known that at sufficiently low beam currents, electron beam temperature effects cause the gains of collective region free-electron lasers to be lower than the predictions of the cold beam theory.[18] The electron beam temperature is related to the relative spread of the beam energy in the parallel direction and measures as $k\lambda_D$. The spread in the beam energy is mainly due to the quivering motion and the radial shear motion of the electron. In this study, the scattering parameter, $k\lambda_D$, con-

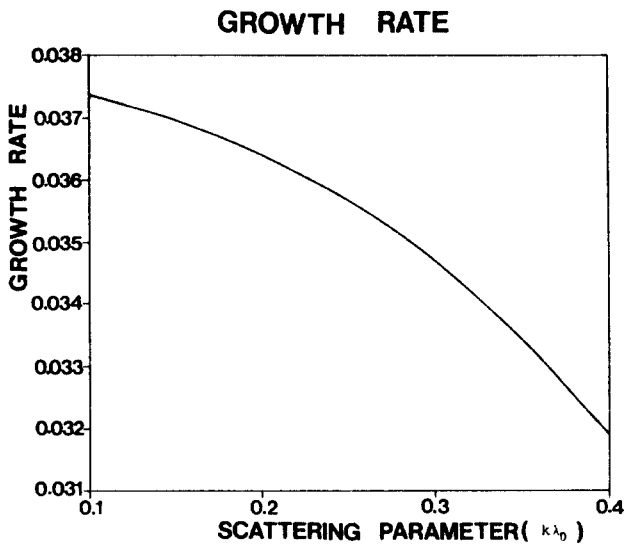

Fig. 2. The spatial growth rate (cm^{-1}) as a function of the scattering parameter ($k\lambda_D$) where $\gamma=1.72$, $B_{0z}=5.54$ KG, F=0.5 and $V_0/c=0.1$.

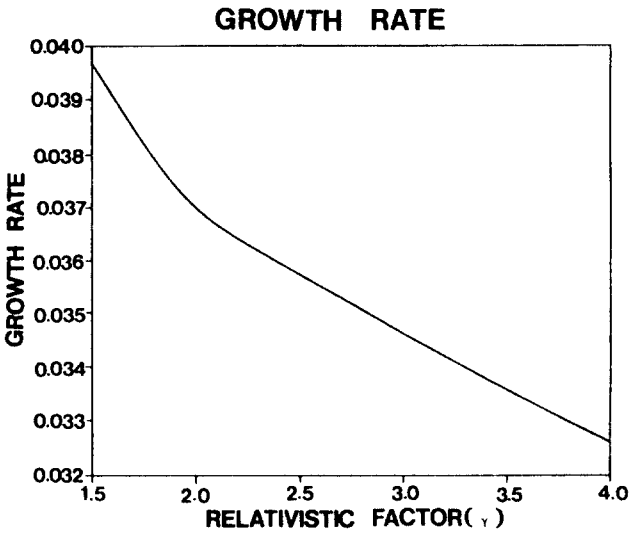

Fig. 3. The spatial growth rate (cm^{-1}) as a function of the relativistic factor where $k\lambda_D=0.1$ $B_{0z}=5.54$ KG, $F=0.5$ and $V_0/c=0.1$.

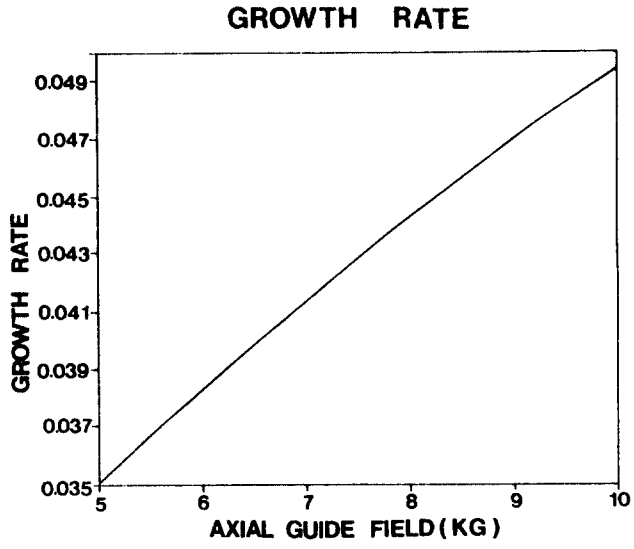

Fig. 4. The spatial growth rate (cm^{-1}) as a function of the magnitude of the axial guide field where $\gamma=2.0$, $k\lambda_D=0.1$, $F=0.5$ and $V_0/c=0.1$.

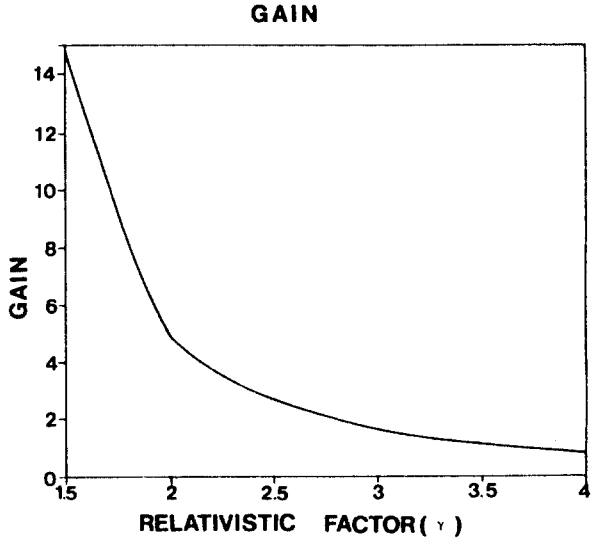

Fig. 5. The gain coefficient as a function of the relativistic factor γ where $B_{0z}=5.54$ KG, $k\lambda_D=0.1$, $V_0/c=0.1$ and $F=0.5$.

tains the temperature effect. We described the thermal effects in the fluid dispersion analysis in terms of a fluid pressure. This is only valid in the Raman scattering region in which the collective wave-wave interaction plays a dominant role in the radiation mechanism.[19] In Fig. 2, we can note that as the beam temperature rises, the spatial growth rate decreases. This is in agreement with previous works.[18,20] As can be seen from Eq. (22a), the growth rate is proportional to the strength of the pump wave. The electron temperature is also proportional to the strength of the pump.[18] Therefore, some saturation of the growth rate is expected, and using the cold beam results as a basis for comparison, we can estimate the electron beam temperature for a given experiment.[18]

Figures 3 and 4 represent the variation of the spatial growth rate with the electron beam energy and the strength of the axial guide field, respectively. The spatial growth rate shows a slight decrease with increasing beam energy and a slight increase with increasing axial guide field.

Next, we plot the gain coefficient formulated by the Madey theorem in Seciton III. In Fig. 5, we can note that the gain coefficient decreases with increasing beam energy. Figure 6 represents the variation of the gain coefficient with the magnitude of the axial guide field.

Finally, we estimate the intrinsic efficiency of energy extraction. In order to assess its efficiency, it is necessary to determine its nonlinear properties. As the wave

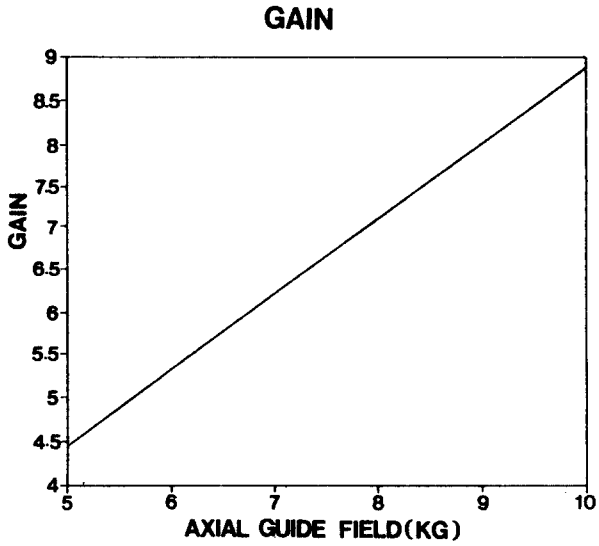

Fig. 6. The gain coefficient as a function of the magnitude of the axial guide field where $\gamma=2.0$, $k\lambda_D=0.1$, $V_0/c=0.1$ and $F=0.5$.

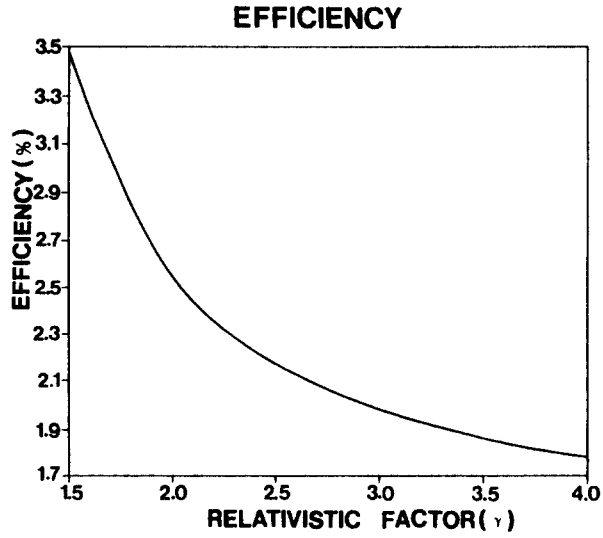

Fig. 7. The efficiency of energy extraction as a function of the relativistic factor γ where $B_{0z}=5.54$ KG, $k\gamma_D=0.1$, $V_0/c=0.1$ and $F=0.5$.

grows and the beam loses energy during the instability, it will eventually reach an amplitude at which it can trap most of the electrons in the beam. After the trapping process sets in, the instability eventually saturates. At this time, the electron beam is, on the average, slowed down to the phase velocity of the ponderomotive wave. Assuming all the energy loss from the electron beam to be converted into electromagnetic radiation, the efficiency, η, is approximately given by[19]

$$\eta=\frac{\gamma_0-\gamma_{ph}}{\gamma_0-1}$$

where $\gamma_{ph}=[1-(\frac{v_{ph}}{c})^2]^{-\frac{1}{2}}$ and $v_{ph}=\frac{\omega_n-\omega_0}{k}$ is the phase velocity of the ponderomotive wave. Figure 7 illustrates the dependence of η on the relativistic factor.

The parameters chosen for use in the figures pertain to region presently realizable in the laboratory. The values of the spatial growth rate obtained is quite low, and this implies the e-folding length for the parametric instability is quite large (~30 cm). The parameters employed here pertain to an on-going experiment[21] in which the relativistic plasma frequency is 2 GHz and the relativistic cyclotron frequency is 9 GHz. However, the larger axial guide filed and electron beam energy would produce a shorter wavelength radiation and e-folding length. Also, we note that as the intensity level of the radiation becomes higher, the spatial growth rate increases. The gain coefficient turns out to have appreciable values for the model parameters chosen in this study. These facts show good promise for the stimulated cyclotron resonance scattering mechanism as a source of tunable, coherent and powerful radiation.

V. SUMMARY

This paper treats the dispersion of the electromagnetic wave and the gain of a free-electron laser which uses an electromagnetic wiggler. We employ the standard stability analysis using the Maxwell fluid equations for the dispersion and the Madey theorem for the gain. Comparing with previous studies,[1-4] the principal contribution of this study is the use of a fluid pressure to treat the effect of beam thermal spread. Besides, we consider the two-dimensional effect by introducing the filling factor, and we formulate the equations in the relativistic region. Thus, we can adequately describe the dispersion of the plasma wave and the *em* wave in the Raman region. Using the obtained results, we can investigate the effects of the operating parameters (the electron beam energy and thermal spread, and the strength of the axial guide field) on the system characteristics (spatial growth rate, gain, and efficiency). This visualization is performed under the model parameters of on-going experiments.

ACKNOWLEDGEMENT

This work was supported by the Korea Research Foundation.

REFERENCES

[1] P. Sprangle and V. L. Granatstein, Appl. Phys. Lett. **25**, 377 (1974).
[1] P. Sprangle, V. L. Granatstein and L. Baker, Phys. Rev. **A12**, 1697 (1975).
[3] A. Goldring and L. Friedland, Phys. Rev. **A32**, 2879 (1985).
[4] H. P. Freund, R. A. Kehs and V. L. Granatstein, Phys. Rev. **A34**, 2007 (1986).
[5] N. M. Kroll and W. A. McMullin, Phys. Rev. **A17**, 300

(1978).
[6] B. G. Danly et al., IEEE J. of Quant. Electron. **QE-23**, 103 (1987).
[7] L. R. Elias, Phys. Rev. Lett. **42**, 977 (1979).
[8] I. Kimmel, L. R. Elias and G. Ramian, Nucl. Instr. and Meth. **A250**, 320 (1986).
[9] J. Gea-Banacloche, G. Moore, R. Schicher, M. Scully and H. Walther, IEEE J. of Quant. Electron. **QE-23**, 1558 (1987).
[10] J. A. Pasour, Proc. SPIE **738**, 55 (1987).
[11] T. H. Chung, Ph. D. thesis, University of Michigan (1986).
[12] J. M. J. Madey, Nuovo Cimento **50B**, 64 (1979).
[13] Han S. Uhm and R. C. Davidson, Phys. Fluids **26**, 288 (1983).
[14] R. C. Davidson, *Theory of Nonneutral Plasmas* (Benjamin Reading , MA, 1974).
[15] G. Schmidt, *Physics of High Temperature Plasmas* (Academic Press, New York, 1979), p. 46.
[16] L. K. Grover and R. H. Pantell, IEEE J. of Quant. Electron. **QE-21**, 944 (1985).
[17] K. Mima et al., Nucl. Instr. and Methods in Phys. Research **A272**, 106 (1988).
[18] J. Fajans and G. Bekefi, IEEE J. of Quant. Electron. **QE-23**, 1617 (1987).
[19] T. Kwan and J. M. Dawson, Phys. Fluids **22**, 1089 (1979).
[20] L. F. Ibanez and S. Johnston, IEEE J. of Quant. Electron. **QE-19**, 346 (1983).
[21] J. Masud et al., Phys. Rev. Lett. **58**, 763 (1987).